JOURNAL OF THE AMERICAN CHEMICAL SOCIETY

Subscriber access provided by EAST TENNESSEE STATE UNIV

Article

Powering a CO_2 Reduction Catalyst with Visible Light through Multiple Sub-picosecond Electron Transfers from a Quantum Dot

Shichen Lian, Mohamad S. Kodaimati, Dmitriy S. Dolzhnikov, Raul Calzada, and Emily A. Weiss

J. Am. Chem. Soc., **Just Accepted Manuscript** • Publication Date (Web): 13 Jun 2017

Downloaded from http://pubs.acs.org on June 13, 2017

Just Accepted

“Just Accepted” manuscripts have been peer-reviewed and accepted for publication. They are posted online prior to technical editing, formatting for publication and author proofing. The American Chemical Society provides “Just Accepted” as a free service to the research community to expedite the dissemination of scientific material as soon as possible after acceptance. “Just Accepted” manuscripts appear in full in PDF format accompanied by an HTML abstract. “Just Accepted” manuscripts have been fully peer reviewed, but should not be considered the official version of record. They are accessible to all readers and citable by the Digital Object Identifier (DOI®). “Just Accepted” is an optional service offered to authors. Therefore, the “Just Accepted” Web site may not include all articles that will be published in the journal. After a manuscript is technically edited and formatted, it will be removed from the “Just Accepted” Web site and published as an ASAP article. Note that technical editing may introduce minor changes to the manuscript text and/or graphics which could affect content, and all legal disclaimers and ethical guidelines that apply to the journal pertain. ACS cannot be held responsible for errors or consequences arising from the use of information contained in these “Just Accepted” manuscripts.

ACS Publications

Journal of the American Chemical Society is published by the American Chemical Society. 1155 Sixteenth Street N.W., Washington, DC 20036

Published by American Chemical Society. Copyright © American Chemical Society. However, no copyright claim is made to original U.S. Government works, or works produced by employees of any Commonwealth realm Crown government in the course of their duties.

Powering a CO_2 Reduction Catalyst with Visible Light through Multiple Sub-picosecond Electron Transfers from a Quantum Dot

Shichen Lian, Mohamad S. Kodaimati, Dmitriy S. Dolzhnikov, Raul Calzada, and Emily A. Weiss*

Department of Chemistry, Northwestern University, 2145 Sheridan Rd., Evanston, IL 60208-3113

*corresponding author. Email: e-weiss@northwestern.edu

ABSTRACT

Photosensitization of molecular catalysts to reduce CO_2 to CO is a sustainable route to storable solar fuels. Crucial to the sensitization process is highly efficient transfer of redox equivalents from sensitizer to catalyst; in systems with molecular sensitizers, this transfer is often slow because it is gated by diffusion-limited collisions between sensitizer and catalyst. This article describes the photosensitization of a *meso*-tetraphenylporphyrin iron(III) chloride (FeTPP) catalyst by colloidal, heavy metal-free $CuInS_2$/ZnS quantum dots (QDs) to reduce CO_2 to CO using 450-nm light. The sensitization efficiency (turnover number per absorbed unit of photon energy) of the QD system is a factor of 18 greater than that of an analogous system with a *fac*-tris(2-phenylpyridine)iridium sensitizer. This high efficiency originates in ultrafast electron transfer between the QD and FeTPP, enabled by formation of QD/FeTPP complexes. Optical spectroscopy reveals that the electron transfer processes primarily responsible for the first two sensitization steps ($Fe^{III}TPP \rightarrow Fe^{II}TPP$, and $Fe^{II}TPP \rightarrow Fe^{I}TPP$) both occur in <200 fs.

INTRODUCTION

Photocatalytic reduction of CO_2 is a sustainable way to utilize abundant solar energy to produce CO, a precursor for reactions that form storable H_2 and liquid fuels, such as the water-gas shift and Fischer-Tropsch processes, and reactions using organometallic complexes that run under much milder conditions.[1-3] Several molecular redox catalysts, containing precious metals such as Re[4-6] or earth-abundant metals such as Co[7,8], Ni[9,10], and Fe[11,12], are capable of reducing CO_2 to CO electrochemically or photochemically. *Meso*-tetraphenylporphyrin iron(III) chloride (FeTPP) and its derivatives are the class of earth-abundant homogeneous catalysts with the best combination of efficiency and chemical stability for the reduction of CO_2 to CO, when they are fed electrons by an electrode or photosensitizer,[13-15] such as tris(bipyridine)ruthenium(II) chloride ($Ru(bpy)_3$), *fac*-tris(2-phenylpyridine)iridium ($Ir(ppy)_3$), or organic dye.[16-18] These sensitizers, however, either contain precious metals or only absorb a significant amount of light at 400 nm or shorter wavelengths (which only accounts for ~4% of the photons in the AM 1.5G solar spectrum). Furthermore, without extensive organic synthesis to covalently link sensitizer with catalyst[19,20], these sensitizers do not have a mechanism for chemisorption of photosensitizers and catalysts. The electron transfer between the two is then primarily mediated by bimolecular collision reactions, with rates and catalytic efficiencies limited by diffusion and concentration.[14,21] A final disadvantage of these sensitizers is that adjusting their redox potentials or absorption spectra to accommodate a certain application or catalyst, by changing the coordination environments of metals or the size of the π systems of organics, is not straightforward synthetically, and often results in sacrificing one desirable property – coverage of the solar spectrum, electrochemical potential, or chemical stability – for another.

Colloidal quantum dots as photosensitizers for CO_2 reduction offer solutions to all of these problems. The heavy metal-free $CuInS_2$/ZnS core/shell QDs we use in this study have an extinction coefficient of ε = ~70000 $M^{-1}\cdot cm^{-1}$ at 450 nm, a factor of 3 - 25 greater than that of $Ir(ppy)_3$ and $Ru(bpy)_3$, **Figure 1A**.[22-24] Quantum confinement of their electrons renders their absorption spectrum tunable over the visible region by simply changing their diameter, and enhances their reduction potential from -1.7 V for bulk $CuInS_2$ [25] to ~ -2.4 V *vs.* SCE for the QDs we use here (diameter = 2.5 nm, **Figure 1B**), enough to perform all three reductions of FeTPP required for CO_2 binding and reduction. Importantly, QDs also have large surface area-to-volume ratios, and their surfaces facilitate (or can be simply functionalized to facilitate)[26-31] the adsorption of molecular catalysts to form quasi-static complexes that mediate femtosecond-to-picosecond rather than microsecond (diffusion-limited) charge transfer between sensitizer and catalyst.[32]

The two reports of catalytic systems using heavy-metal containing CdS QDs as photosensitizers for CO_2 reduction (with enzyme[33] and cobalt complex co-catalysts[34]) show promise for this strategy, but both had energy efficiencies limited by the reduction potential of CdS QDs, which are approximately 1 V less reducing than $CuInS_2$, and by their limited absorption of visible light.[35] Feldmann and co-workers demonstrated the efficacy of a combination of more highly reducing Cu_2S nanorods with Pt nanoparticles for conversion of CO_2 to CO and methane, although the 1.2 eV bandgap of Cu_2S required an exceptional hole scavenger.[36]

Here we show that soluble, colloidal, heavy metal-free $CuInS_2$/ZnS QDs photosensitize the catalytic conversion of CO_2 to CO by a model catalyst, FeTPP, in DMSO, using visible light, **Scheme 1**. Upon successive photoexcitations at 450 nm, the QD donates three electrons – the first and second in <200 fs – to form the catalytically active species Fe^0TPP, which binds CO_2 and reduces it to CO with 84% selectivity (16% H_2). The sacrificial reductant *N,N,N′,N′*-tetramethyl-*p*-phenylenediamine (TMPD) re-establishes the QD's ground state within 700 ps. There is no detectable degradation of catalytic activity over 40 h, the longest time we monitored the system. The sensitization efficiency of this sensitizer-catalyst system is a factor of 18 higher than the most efficient photostable homogenous system for photoreduction of CO_2 to CO using an earth abundant metal, $FeTPP(OH)_4$ sensitized by $Ir(ppy)_3$,[14] even though $Ir(ppy)_3$ absorbs higher-energy light (420 nm) than does the QD. Mechanistic analysis of the photosensitizer-catalyst interaction is crucial for maximizing what in electrocatalysis is the "heterogeneous rate constant", the rate of injection of redox equivalents into the catalyst. This type of analysis is often complicated with, for example, $Ir(ppy)_3$ or $Ru(bpy)_3$, sensitizers because these complexes form triplet excited states, undergo intramolecular charge separations, and have convoluting ground-state absorption features with the molecular co-catalysts. The QDs that we use here allow for direct measurements of the rates for photoinduced electron transfer. Specifically, time-resolved optical spectroscopy allows us to determine the origin of the high efficiency of the QD-FeTPP system: ultrafast electron donation from the QD to FeTPP in near-quantitative yield, enabled by the formation of quasi-static complexes of sensitizer and catalyst with no covalent linking chemistry.

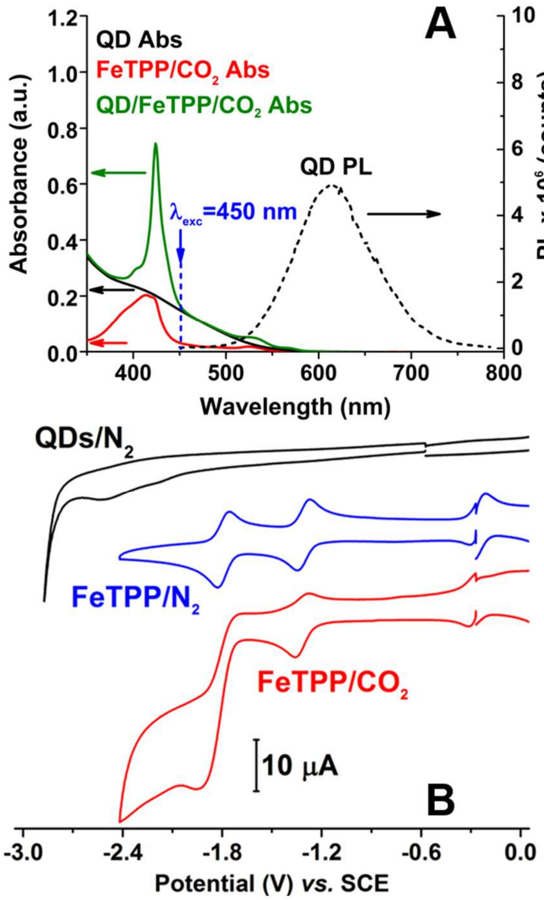

Figure 1. Characterization of the Catalyst and Sensitizer. A) Ground state absorption spectra of 16 µM $CuInS_2/ZnS$ core/shell QDs (black), 8 µM FeTPP purged with CO_2 (red), and a mixture of the QDs and 0.5 eq. FeTPP purged with CO_2 (green); and PL spectrum of the QDs (black dash), in DMSO. The blue arrow indicates the excitation wavelength used for the catalysis, PL, and transient absorption experiments. **B)** CV of 1 mM QDs under N_2 (black), FeTPP under N_2 (blue), and FeTPP under CO_2 (red), with 50 mM tetrabutylammonium hexafluorophosphate in DMSO, a glassy carbon working electrode, an Ag wire reference electrode, and a Pt wire counter electrode. The potentials have been referenced to SCE using a ferrocene internal standard. The discontinuities in the scans are artifacts caused by switching the polarity of the electrodes (shifted below 0 V when referencing the data to Fc/Fc^+).

RESULTS AND DISCUSSION

Catalytic Mixture and Mechanism. We synthesized oleate-capped $CuInS_2/ZnS$ core/shell QDs based on a modified literature procedure[37] (Figure S11) and subsequently displaced all of the oleate ligands (as shown by NMR, see Figure S1) with 3-mercapto-1-propanol (MPO) to form DMSO-soluble QDs, the photosensitizers for the reaction. The Supporting Information describes our synthesis and ligand exchange procedure in detail.

Figure 1A shows that the broad first excitonic peak of MPO-capped $CuInS_2$ QDs is centered near 435 nm, and the emission peaks at 610 nm, which corresponds to a particle diameter of 2.5 nm.[22] Upon introduction of QDs, the Soret band of FeTPP shifts to lower energy, which suggests a change in axial ligand substitution, specifically that the Fe center within FeTPP is interacting with an electron donating group[38,39] (probably the electron-enriched sulfur sites on the surface of QDs)[40]. When the QDs are mixed with FeTPP in CO_2-saturated DMSO, in the molar ratio used for the catalysis (QD:FeTPP = 1:0.02) or that used for the time-resolved spectroscopy experiments (QD:FeTPP = 1:0.5), we achieve excellent selectivity (≥95%) for photoexcitation of the QD sensitizer (as opposed to FeTPP) at 450 nm, the excitation wavelength used for all studies, **Figure 1A** (green). We use a large excess of QD sensitizer for catalysis in order to ensure that at most one FeTPP binds per QD, and thereby maximize the probability that photoexcited electrons all go to the same catalyst.

Figure 1B shows cyclic voltammograms (CVs) of MPO-capped QDs under N_2, FeTPP under N_2, and FeTPP under CO_2, all in DMSO. When the FeTPP sample is purged with CO_2, catalytic current is observed upon reduction of Fe^+ to Fe^0, which confirms that the Fe^0 center within FeTPP molecule is the catalytic site.[13,14] The first observed reductive wave of the QDs (~-2.5 V) is more negative than the catalyst standard potential, which indicates that the photoinduced electrons within $CuInS_2$ QDs used in this study have enough energy to reduce Fe^{III} to Fe^0, and thereby photosensitize FeTPP.

Scheme 1. Proposed Photocatalytic Mechanism for the Reduction of CO_2 to CO *via* Electron Transfer from the QD to FeTPP and Hole Transfer from the QD to TMPD.

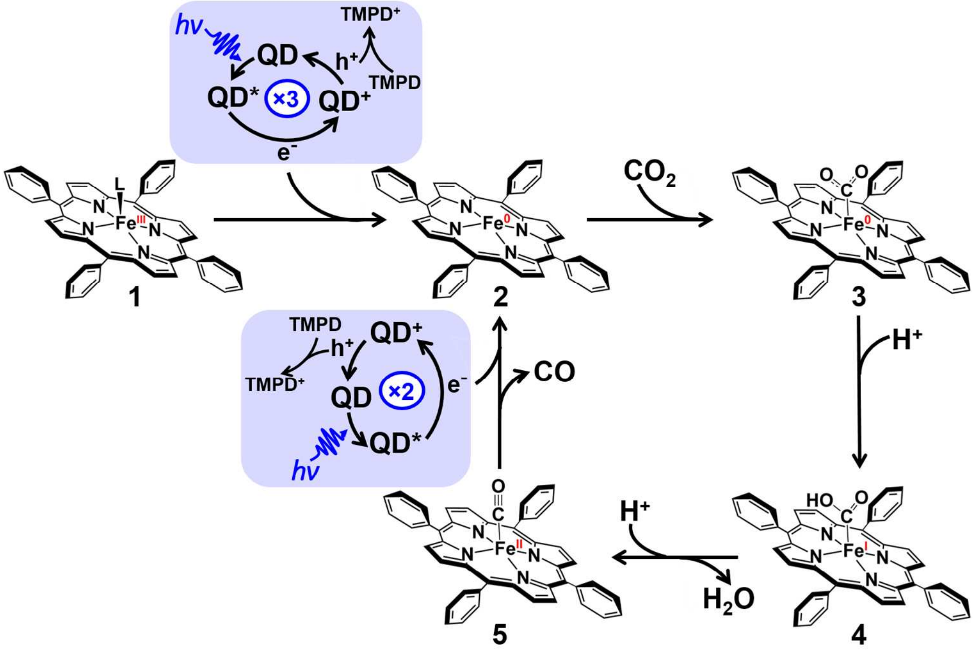

Scheme 1 summarizes a photocatalytic mechanism for CO_2 reduction by QD-sensitized FeTPP, based on the previously reported electrochemical mechanism.[41] During the initial sensitization step (top blue shaded region), a QD sequentially accepts three photons, one at a time. After each photoexcitation (to form QD*), the QD donates one electron to FeTPP and one

hole to the sacrificial reductant, TMPD, to regenerate its ground state. The Fe^{III} center within **1** thereby consecutively accepts three electrons to become Fe^0 (**2**), which binds CO_2 to form the catalytically active species Fe^0-$C^{(+4)}O_2$ (**3**). The first step of the reduction of CO_2 is a proton-coupled electron transfer (PCET) from Fe^0 to CO_2 to form Fe^I-$C^{(+3)}OOH$ (**4**). The $C^{(+3)}OOH$ moiety in **4** then accepts another electron from Fe^I and another proton from the surrounding media and undergoes dehydration to form **5**. Finally, a CO molecule releases from **5**. In another sensitization step, the remaining Fe^{II} center captures two electrons from a consecutively photoexcited QD to re-establish **2** and continue the catalytic cycle. We suspect that the ligand "**L**" in **1** is DMSO when CO_2 is not present, and is CO_2 (although the exact nature of binding mode is unclear) when it is available, because, upon addition of CO_2 to FeTPP, changes in the absorption spectrum of FeTPP, possibly indicative of axial ligand substitution, occur, see the Figure S2.[39]

We suspect, but have not proven, that the protons needed during this cycle are donated by residual water in the DMSO (which we did not dry thoroughly) and the water formed during the ligand exchange procedure. During the phase transfer of the QDs to DMSO, we added benzyltrimethylammonium hydroxide (triton B) to deprotonate the added thiols (the MPO ligands) to thiolates. This process generates water, which is then transferred to DMSO.

Catalytic Efficiency of the QD-FeTPP Mixture. The Methods section describes our photocatalytic setup in detail. Briefly, we put QDs samples in air-tight vials and illuminated these vials with a 4.5-mW, 450 nm laser pointer (bandwidth = ~ 2 nm) for various amount of time. We then sampled the head space of these vials with gas chromatography (GC) with thermal conductivity detection (TCD) to monitor the production of H_2 and CO. ^1H NMR of the samples in DMSO-d_6 did not detect any solution-phase catalytic products. Without light, the QD/FeTPP/CO_2 sample does not produce any CO or H_2. After 10 hours of illumination at 450 nm, the QD/FeTPP/CO_2 mixture produces both H_2 and CO, whereas the QD/FeTPP/Ar mixture produces only a trace amount of H_2. With no added FeTPP, the QD/CO_2 sample produces primarily H_2 and a negligible amount of CO. The FeTPP/CO_2 sample (with no QDs) under the same conditions does not produce a GC-detectable amount of H_2 or CO (see all GC traces in Figure S3). Qualitative analysis of the GC data allows us to conclude that i) the detected CO is coming from CO_2, not from another carbon source such as the surface ligands or solvent, ii) the electrons that reduce the Fe center in FeTPP originate from the photoexcited state of the QD, and

iii) the vast majority of CO is produced by the QD/FeTPP assembly, rather than by the QD or FeTPP on its own.

Figure 2, red triangles, shows the kinetics of CO production for our reaction mixture, $CuInS_2$ QDs with 0.02 eq. FeTPP, 1000 eq. of the hole scavenger TMPD, in DMSO purged with CO_2. The QD/FeTPP system shows no sign of decreasing catalytic activity after 40 hours of illumination at 450 nm and 4.5 mW (Figure S8). Our goal is to demonstrate and analyze the effectiveness of our QD-based sensitization scheme for the particular FeTPP catalyst we have chosen – that is, the efficiency with which the QD transduces light energy to reducing equivalents, and ultimately to CO. The conventional plot of turnover number (TON = [CO]/[catalyst]) *vs.* illumination time does not, however, account for the intensity or energy of the light source (a higher photon flux, for example, will lead to more CO by creating more redox equivalents per unit time) and is therefore not a good measure of sensitization efficiency. Instead, we plot in **Figure 2** (red triangles) the TON vs. cumulative photon energy absorbed by the sensitizer, calculated according to **eq. 1**. Also

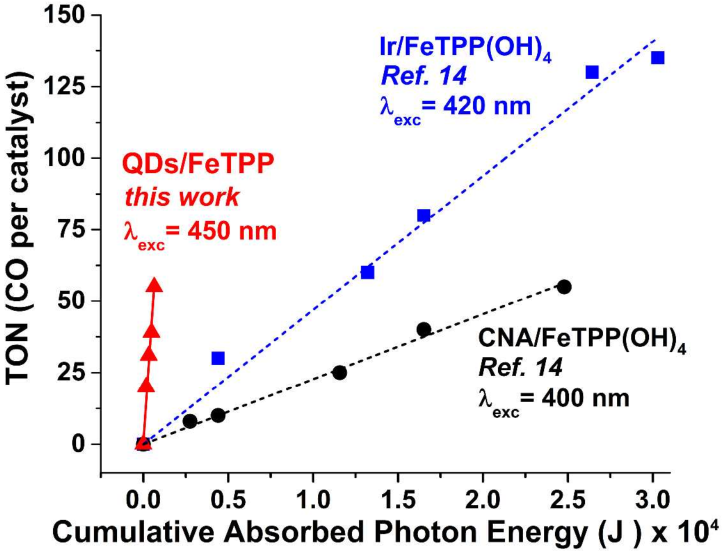

Figure 2. Measurement of Catalytic Efficiency. Red triangles: Plot of the turnover number of CO (per catalyst molecule) *vs.* the cumulative absorbed photon energy, upon illumination of a mixture of 100 μM QDs (+ 1000 eq. TMPD) and 2 μM of FeTPP in CO_2-saturated DMSO. Shown for comparison are analogous data (extracted from *Ref.14*) for the production of CO by a hydroxylated FeTPP catalyst, photosensitized by $Ir(ppy)_3$ (blue squares) or CNA (black circles), as described in the text. The Supporting Information contains the GC traces used to construct this plot and the calculation of cumulative input photon energy from illumination time.

$$Cumulative\ absorbed\ photon\ energy\ (J) = light\ intensity\ \left(\frac{J}{s * cm^2}\right) \times illumination\ area\ (cm^2) \times time(s) \times fraction\ of\ photons\ absorbed \qquad (1)$$

plotted in **Figure 2** are the analogous datasets for two published photocatalytic reaction mixtures: a derivatized FeTPP catalyst sensitized by Ir(ppy)$_3$ (blue squares) and by 9-cyanoanthracene (CNA, black circles). We chose these data for comparison because Ir(ppy)$_3$ is the most commonly used photosensitizer for all molecular-catalyst based homogenous photoreduction of CO$_2$, and because FeTPP(OH)$_4$/Ir(ppy)$_3$ is the most efficient photostable homogenous system for photoreduction of CO$_2$ to CO. The combination of several other Fe^{II} and Co^{II} based catalysts coupled with Ir(ppy)$_3$/Ru(bpy)$_3$ sensitizers[21,42-45] have higher turnover frequencies, but all have turnover number vs. time plots that deviate from linearity within ten hours of illumination, indicating some degradation or poisoning of the catalytic system. In constructing the plots in **Figure 2**, we assume the TON is photon-limited – that is, increasing the power of the excitation source will increase the total amount of CO produced; we prove this assumption for both our system and the published systems, and show our detailed calculations using **eq 1**, in the Supporting Information.

The sensitization efficiency (defined as *the number of CO molecules produced / J of absorbed photon energy / catalyst molecule*, i.e. the slope of the curve in **Figure 2**) of the QD-sensitized system is a factor of 18 larger than that of Ir-sensitized system, and a factor of 38 larger than that of the CNA-sensitized system. Given the data in **Figure 2**, the external quantum efficiency for conversion of photons to reducing equivalents, *EQE* = *2×(number of CO molecules produced per catalyst)/(number of incident photons),* is 0.01% for the QD-sensitized system, 0.0013% for the Ir-sensitized system, and 0.0008% for the CNA-sensitized system.[14 46]

Importantly, the enhancement in sensitization efficiency by the QDs, relative to Ir and CNA, is much more dramatic than what is evident from **Figure 2** and the numbers we derive from it, because in order to compare our system to the Ir and CNA-sensitized systems, we ignored two important features of the published systems that *overestimates* their performance relative to that of the QD-sensitized system. First, the catalyst used in the Ir- and CNA-sensitized systems is (FeTPP(OH)$_4$), whereas we use FeTPP. The hydroxyl groups of (FeTPP(OH)$_4$) stabilize the CO$_2$-FeTPP species through hydrogen bonding, resulting in a decrease of the overpotential for reduction of CO$_2$ to CO by up to 0.4 V and an increase in the rate constant for catalysis (in their electrochemical experiment) by a factor of 100.[13] Second, we use a monochromatic (450-nm) laser pointer as a light source, so the energy input plotted on the *x*-axis of **Figure 2** is the *only* energy we use to produce CO. In contrast, the authors of the published Ir and CNA work (and almost all studies on the photoreduction of CO_2) used a broadband light source, and the turnover numbers plotted in **Figure 2** for their systems are a result of energy absorbed by their sensitizers over a range of wavelengths. Since we do not, however, know the intensity profile of their lamp, we calculated the energy input plotted on the *x*-axis of **Figure 2** only from the single wavelength at which they reported the power of their incident light, when in fact more energy was absorbed at other wavelengths. Due to both this discrepancy and the difference in catalyst between our experiment and the published experiment, **Figure 2** only shows the lower limit of the enhancement in sensitization efficiency by the QDs, relative to the best known photostable sensitizers for FeTPPs. Interestingly, when we mixed $Ir(ppy)_3$ with FeTPP (instead of the hydroxylated FeTPP used in *ref 14*), we observed the formation of H_2 and no CO at all (Figure S12 in the Supporting Information) upon excitation at 405 nm. This result further proves that QDs can photosensitize FeTPP for the reduction of CO_2 much more efficiently than $Ir(ppy)_3$ under similar illumination conditions and that production of CO using the $Ir(ppy)_3$ sensitizer requires the “better” (hydroxyl-functionalized) FeTPP catalyst.

The catalytic selectivity for formation of CO over H_2, $[CO]/([CO] + [H_2])$, of the QD/FeTPP system is 84%, Figure S8, slightly lower than the selectivities of the $Ir(ppy)_3/FeTPP(OH)_4$ (93%) and $CNA/FeTPP(OH)_4$ (100%) systems. We suspect that the H_2 in our system is produced *via* direct reduction of H^+ by photoexcited QDs without adsorbed FeTPP, since we only used 0.02 eq. FeTPP per QD and the possible proton source includes the residual water in DMSO and leftover water generated during ligand exchange procedure (see the Supporting Information for details). Further optimization of the sensitizer:catalyst ratio should allow us to increase the selectivity of our system.

Efficient photosensitization is enabled by ultrafast electron transfer (eT) from QDs to FeTPP. Why are the QDs more efficient sensitizers for FeTPP than the Ir and CNA systems, both in terms of quantum efficiency and energy efficiency? One immediate advantage of the $CuInS_2$ QD system is that it can be photoexcited at longer wavelengths than the Ir and CNA sensitizers and still produce sufficiently reducing electrons. This feature of $CuInS_2$ QDs is also advantageous, in general, for minimizing side reactions that occur more frequently with higher-energy incident photons. The more subtle, and more important, advantage of the QD-sensitized system is that, while the exceptionally low yields of PL quenching of the sensitizer in molecular systems like Ir/FeTPP(OH)$_4$ and CNA/FeTPP(OH)$_4$ strongly suggest that eT in these systems relies on collisions between freely diffusing sensitizers and catalysts to transfer electrons between the two (Figure S9 of the Supporting Information), such that the eT is gated by bimolecular reaction kinetics, the QDs and FeTPP form what appears to be high-affinity sensitizer/catalyst complexes. Again, the formation of these complexes is supported by the spectral shift of the Soret band of FeTPP upon addition of QDs (**Figure 1A,** green *vs*. red).

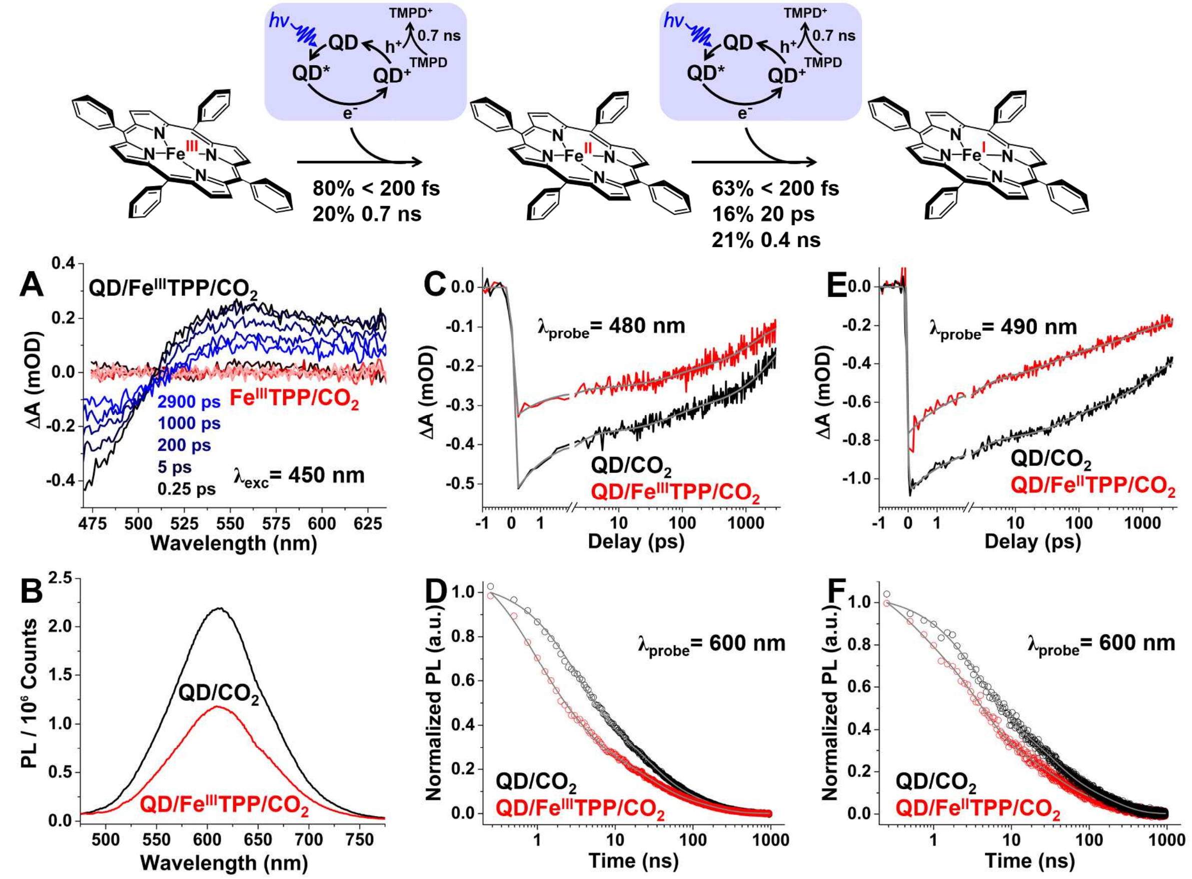

Figure 3. Kinetics of Photoreduction of the Catalyst by the QD Sensitizer. A) TA spectra of FeTPP (light red→dark red), or a mixture QDs and of Fe^{III}TPP (black → blue), at various delay times after excitation at 450 nm. Fe^{III}TPP/CO$_2$ itself has no transient absorptions or bleaches in this region. **B)** Steady-state PL spectra of the QDs without (black) and with (red) added Fe^{III}TPP. The integrated PL intensity of the QDs is quenched by 45% upon addition of 0.5 eq. of Fe^{III}TPP. **C)** Kinetic traces extracted at 480 nm from the TA spectra of the QDs (black) and a mixture QDs and of Fe^{III}TPP (red), after excitation at 450 nm. The dynamics at these wavelengths are those of the reducing electron of the QD. **D)** Decay of the PL of QDs without (black) and with (red) added Fe^{III}TPP, monitored at 600 nm, after excitation at 450 nm. **E)** Kinetic traces extracted at 490 nm from the TA spectra of the QDs (black) and a mixture QDs and of Fe^{II}TPP (red). This set of TA experiments was conducted with excitation at 460 nm in order to selectively excite the QDs. Fe^{II}TPP does not attenuate any light at this wavelength. **F)** Decay of the PL of QDs without (black) and with (red) added Fe^{II}TPP, monitored at 600 nm, after excitation at 450 nm. Tables 1-3 list the fitting parameters for the TA and PL data. All samples are in DMSO and purged with CO$_2$. All mixtures of QDs and FeTPP have 0.5 eq. FeTPP per QD. The two kinetic traces in each of (**C**) and (**E**) were collected with the same excitation power and pump-probe overlap, so their amplitudes are comparable at all delay times.

The consequence of the formation of these sensitizer-catalyst complexes is significant electronic coupling of the QD and FeTPP and, we show here, ultrafast reduction of the catalyst by the QD. Upon addition of 0.5 eq. of FeTPP to the QDs, the photoluminescence (PL) intensity of the QDs is quenched by 45%, **Figure 3B**, a quenching yield of 90% (quenching yield = $\frac{\%\ of\ PL\ quenching}{molar\ ratio\ of\ FeTPP:QD}$). Given that we know that (i) QDs reductively photocatalyze the production of CO *via* the FeTPP catalyst (**Figure 2**), and (ii) eT from the QDs to Fe^{III}TPP is thermodynamically favorable (**Figure 1B**), whereas hole transfer (which would produce QD^--Fe^{IV}-TPP) and energy transfer (which requires spectral overlap between the emission of QDs and the absorption of FeTPP) are not, we can confidently conclude that the quenching mechanism is eT from QDs to FeTPP. The 90% yield for PL quenching indicates that eT from the QD to FeTPP must be fast enough to out-compete nearly all other decay mechanisms for the photoexcited electron.

To measure the rate of the eT process for the initial sensitization step (Fe^{III}TPP → Fe^{II}TPP), we acquired transient absorption (TA) spectra of $CuInS_2$ QDs with 0.5 eq. of Fe^{III}TPP (blue), in DMSO and purged with CO_2, after monochromatic excitation of the system with an ultra-short pulse at 450 nm, **Figure 3A**. We used 0.5 eq. rather than 0.02 eq. of catalyst in this experiment because more QD-catalyst complexes afford more signal, and we are not concerned with the yield of multi-electron transfer, only the rate of the first eT step, from QD* to Fe^{III} to form Fe^{II}. The Supporting Information describes the features of the TA spectra of $CuInS_2$ QDs in detail; here we only say that since (i) the TA spectra of Fe^{III}TPP purged with CO_2, *without* QDs, have no observable features in this region and time window (250 fs - 3 ns) (**Figure 3A**), (ii) the ground state absorption spectra of QDs/CO_2 and QDs/Fe^{III}TPP/CO_2 overlay exactly at 450 nm (**Figure 1A**), and (iii) the amplitude of the ground state bleach feature (GSB, 470 nm – 510 nm) is not sensitive to the excitonic hole[46], we can use the dynamics of GSB of the QDs to selectively monitor the dynamics of reducing electrons in the photoexcited QD. Furthermore, these dynamics will only reflect charge separation, not charge recombination, processes involving the QD.

Figure 3C (black) shows a kinetic trace extracted from the TA spectra of QD/CO_2 samples at a wavelength near the peak of the GSB of the QDs (480 nm). As summarized in Table S1, the recovery of the GSB occurs with at least four distinct exponential processes, which we assign to known excitonic processes of the QD. **Figure 3C** (red) shows a kinetic trace extracted from the TA spectra of QD/Fe^{III}TPP/CO_2 sample at 480 nm. The QD/CO_2 and QD/Fe^{III}TPP/CO_2 samples were prepared using the same QD stock solution, and measured using the same excitation power and pump-probe overlap. The only difference between the two samples is that one has Fe^{III}TPP and the other does not. Since Fe^{III}TPP does not contribute to the TA spectrum in this region (**Figure 3A**), any difference between the amplitudes or dynamics of the signals from the two samples must be related to the response of the QD's photoexcited electron to Fe^{III}TPP. The dynamics of the electron in the QD/ Fe^{III}TPP /CO_2 samples are very similar to those of the QD/CO_2 samples (see Table S1) with one major difference: the initial magnitude of the GSB (at ~200 fs after photoexcitation, the earliest time delay we can measure with our setup) is always smaller upon addition of Fe^{III}TPP. Given the identical conditions of the experiment, this initial depletion of the excited state of the QD must be caused by eT from the QD to Fe^{III}TPP within the instrument response time (IRF~200 fs, Figure S7).[47-50]

This sub-200 fs eT process from the QD to Fe^{III}TPP accounts for a 36% quenching of the QD excited state when complexed with FeTPP, but recall that 45% of the PL of the QD ensemble is quenched upon addition of FeTPP. The remaining 9% of the quenching can be accounted for quantitatively by eT from QD* to Fe^{III}TPP on a longer timescale (0.7 ns), which we detect by time-correlated single photon counting (TCSPC, **Figure 3D** and Table S2). We therefore conclude that ~80% of the eT from QD* to Fe^{III}TPP occurs within 200 fs, and the remaining 20% occurs within 0.7 ns. This dual-timescale charge transfer is commonly reported in studies of QD-molecule complexes as molecules can have several binding geometries on the surface of QDs that will result in different magnitudes of electronic coupling.[32] The fact that both eT processes occur in <1 ns supports our claim that the QD and Fe^{III}TPP form a static complex, even without covalent linking chemistry, because a diffusion-limited process would occur no faster than hundreds of nanoseconds at these concentrations.[51]

We also measured the rate of the second sensitization step, the photoreduction of Fe^{II}TPP to Fe^{I}TPP by the QDs, by mixing QDs with the catalyst pre-reduced to Fe^{II} by cobaltocene. The Supporting Information contains the details for this experiment, controls, and characterization of Fe^{II}TPP. Addition of 0.5 eq. of Fe^{II}TPP again quenches the PL intensity of the QD with an efficiency of ~90 % (Figure S4). TA (**Figure 3E** and Table S3) and TCSPC (**Figure 3F** and Table S4) analyses of the QD/Fe^{II}TPP assembly reveals that 63% of eT from QD^{*} to Fe^{II}TPP occurs within 200 fs, 16% occurs in ~20 ps, and 21% occurs ~0.4 ns, respectively. Chemically reduced Fe^{I}TPP was too unstable to study eT dynamics in the QD/Fe^{I}TPP assembly;[52] however, a simple Marcus theory analysis predicts that photoreduction of Fe^{I}TPP should be slower than photoreduction of Fe^{II}TPP by only a factor of 5, given the difference in reduction potentials of Fe^{I}TPP and Fe^{II}TPP, see the Supporting Information.

We also used TCSPC to determine that hole transfer from QDs to the sacrificial reductant TMPD occurs in 0.7 ns, see Figure S6 and table S5.

CONCLUSIONS

In summary, colloidal CuInS$_2$/ZnS QDs sensitize FeTPP to reduce CO$_2$ to CO using 450-nm light with a sensitization efficiency, defined as the TON of CO per catalyst per absorbed unit of photon energy, that is a factor of 18 greater than that of an analogous system with an Ir-based organometallic sensitizer. The selectivity for CO is 84% (16% H$_2$). The QD/FeTPP mixture is stable after 40 hours of illumination at 4.5 mW. We have underscored, in this work, that design of effective QD-sensitized catalytic systems, particularly those for multi-electron transfer, must emphasize not only the relative potentials of sensitizer and catalyst, but also their electronic coupling. The efficiency of sensitization in our system originates in the ultrafast electron transfer between the QD and FeTPP: the time constants for the dominant electron transfer processes responsible for the first two sensitization steps (Fe^{III}TPP $\rightarrow$ Fe^{II}TPP, and Fe^{II}TPP $\rightarrow$ Fe^{I}TPP) are both <200 fs. This ultrafast photoreduction is enabled by formation of a quasi-static QD/FeTPP complex, probably driven by the interaction between Fe and sulfur on the surface of the QD. The exact nature of this interaction will require further characterization. The ability of QDs to self-assemble with a co-catalyst is a crucial advantage of the QD-sensitized system over molecular systems, where the rate of charge transfer is limited by occasional collisions between freely diffusing species. Moreover, the methodology we present in this work – the utilization of time-resolved optical spectroscopies to probe the dynamics of individual elementary charge transfer step within the catalytic cycle – is critical for determining the rate-limiting steps within complicated catalytic processes.

Further optimization of our system, such as coupling the QD sensitizer with a more efficient catalyst and tuning the sensitizer:catalyst ratio, will allow us to increase both the quantum efficiency and selectivity of the system for CO. As outlined by Tachibana and coworkers[53], the excitation frequency (i.e., the rate of accumulating photoinduced electrons) is the bottleneck for artificial photosynthesis. Slow rates of absorbing photons for chromophores and short lifetimes of catalytic intermediates are two of the main reasons for low quantum yields in many photocatalytic systems. Designing a system where the chromophores quickly accumulate photoinduced charge carriers and transport them to the catalytic centers is the key for an efficient photocatalytic cell, and the near-unity efficiency of electron transfer from the QD to FeTPP that we achieve here is a good demonstration of this principle. It is also possible to partially substitute or chemically dope $CuInS_2$ to form heterostructures of $CuInS_2$ and a proven water oxidation catalyst such as CoO_4 or $BiVO_4$[54], and thereby both eliminate sacrificial reductants and reduce CO_2 in aqueous media.

Ideally, one would modify the QD surface for high-affinity adsorption of CO_2 in an activated geometry and thereby eliminate the co-catalyst, as achieved by Ozin using hydride-terminated Si QDs exposed to gas-phase CO_2.[55] Direct, selective CO_2 reduction by QDs is however still a work in progress,[56-62] and there is much to be learned and achieved by using QDs to deliver electrons to a known, selective molecular catalyst.

SUPPORTING INFORMATION

Details of QD synthesis, ligand exchange procedures, catalysis setup, GC experiments, ^{1}H NMR, calculations of number of absorbed photons per hour, and time-resolved optical spectroscopy studies. This information is available free of charge via the internet at http://pubs.acs.org.

ACKNOWLEDGEMENT

This work was primarily supported as part of the Argonne-Northwestern Solar Energy Research (ANSER) Center, an Energy Frontier Research Center funded by the U.S. Department of Energy (DOE), Office of Science, Basic Energy Sciences (BES), under Award # DE-SC0001059 (sensitizer synthesis and catalysis studies), and by the National Science Foundation (NSF) under Award # CHE - 1400596 (optical studies). The authors thank Dr. Marek Majewski and Prof. Michael Wasielewski for the use of their GC instrument.

REFERENCES

(1) Hu, Y.; Lee, C. C.; Ribbe, M. W. *Science* **2011**, *333*, 753.
(2) Buss, J. A.; Agapie, T. *Nature* **2016**, *529*, 72.
(3) Summerscales, O. T.; Cloke, F. G. N.; Hitchcock, P. B.; Green, J. C.; Hazari, N. *Science* **2006**, *311*, 829.
(4) Ci, C.; Carbo, J. J.; Neumann, R.; Graaf, C. d.; Poblet, J. M. *ACS Catal.* **2016**, *6*, 6422.

(5) Sahara, G.; Kumagai, H.; Maeda, K.; Kaeffer, N.; Artero, V.; Higashi, M.; Abe, R.; Ishitani, O. *J. Am. Chem. Soc.* **2016**, *138*, 14152.

(6) Nakajima, T.; Tamaki, Y.; Ueno, K.; Kato, E.; Nishikawa, T.; Ohkubo, K.; Yamazaki, Y.; Morimoto, T.; Ishitani, O. *J. Am. Chem. Soc.* **2016**, *138*, 13818.

(7) Zhu, G.; Li, Y.; Zhu, H.; Su, H.; Chan, S. H.; Sun, Q. *ACS Catal.* **2016**, *6*, 6294.

(8) Gao, C.; Meng, Q.; Zhao, K.; Yin, H.; Wang, D.; Guo, J.; Zhao, S.; Chang, L.; He, M.; Li, Q.; Zhao, H.; Huang, X.; Gao, Y.; Tang, Z. *Adv. Mater.* **2016**, *28*, 6485.

(9) Froehlich, J. D.; Kubiak, C. P. *J. Am. Chem. Soc.* **2015**, *137*, 3565.

(10) Thoi, V. S.; Kornienko, N.; Margarit, C. G.; Yang, P.; Chang, C. J. *J. Am. Chem. Soc.* **2013**, *135*, 14413.

(11) Wang, D.; Huang, R.; Liu, W.; Sun, D.; Li, Z. *ACS Catal.* **2014**, *4*, 4254.

(12) Rail, M. D.; Berben, L. A. *J. Am. Chem. Soc.* **2011**, *133*, 18577.

(13) Costentin, C.; Drouet, S.; Robert, M.; Savéant, J.-M. *Science* **2012**, *338*, 90.

(14) Bonin, J.; Robert, M.; Routier, M. *J. Am. Chem. Soc.* **2014**, *136*, 16768.

(15) Rao, H.; Bonin, J.; Robert, M. *Chem. Commun.* **2017**, *53*, 2830.

(16) Kumar, B.; Llorente, M.; Froehlich, J.; Dang, T.; Sathrum, A.; Kubiak, C. P. *Annu. Rev. Phys. Chem.* **2012**, *63*, 541.

(17) Takeda, H.; Cometto, C.; Ishitani, O.; Robert, M. *ACS Catal.* **2017**, *7*, 70.

(18) Arias-Rotondo, D. M.; McCusker, J. K. *Chem. Soc. Rev.* **2016**, *45*, 5803.

(19) Nakada, A.; Koike, K.; Nakashima, T.; Morimoto, T.; Ishitani, O. *Inorg. Chem.* **2015**, *54*, 1800.

(20) Gholamkhass, B.; Mametsuka, H.; Koike, K.; Tanabe, T.; Furue, M.; Ishitani, O. *Inorg. Chem.* **2005**, *44*, 2326.

(21) Guo, Z.; Cheng, S.; Cometto, C.; Anxolabéhère-Mallart, E.; Ng, S.-M.; Ko, C.-C.; Liu, G.; Chen, L.; Robert, M.; Lau, T.-C. *J. Am. Chem. Soc.* **2016**, *138*, 9413.

(22) Booth, M.; Brown, A. P.; Evans, S. D.; Critchley, K. *Chem. Mater.* **2012**, *24*, 2064.

(23) Steinbacher, F. S.; Krause, R.; Hunze, A.; Winnacker, A. *Phys. Status Solidi A* **2012**, *209*, 340.

(24) Lachish, U.; Infelta, P. P.; Grätzel, M. *Chem. Phys. Lett.* **1979**, *62*, 317.

(25) Knowles, K. E.; Hartstein, K. H.; Kilburn, T. B.; Marchioro, A.; Nelson, H. D.; Whitham, P. J.; Gamelin, D. R. *Chem. Rev.* **2016**, *116*, 10820.

(26) Caldwell, M. A.; Albers, A. E.; Levy, S. C.; Pick, T. E.; Cohen, B. E.; Helms, B. A.; Milliron, D. J. *Chem. Commun.* **2011**, *47*, 556.

(27) Tseng, H.-W.; Wilker, M. B.; Damrauer, N. H.; Dukovic, G. *J. Am. Chem. Soc.* **2013**, *135*, 3383.

(28) Knauf, R. R.; Lennox, J. C.; Dempsey, J. L. *Chem. Mater.* **2016**, *28*, 4762.

(29) Waiskopf, N.; Ben-Shahar, Y.; Galchenko, M.; Carmel, I.; Moshitzky, G.; Soreq, H.; Banin, U. *Nano Lett.* **2016**, *16*, 4266.

(30) Williams, E. S.; Major, K. J.; Tobias, A.; Woodall, D.; Morales, V.; Lippincott, C.; Moyer, P. J.; Jones, M. *J. Phys. Chem. C* **2013**, *117*, 4227.

(31) Su, F.; Lu, J.; Tian, Y.; Ma, X.; Gong, J. *Phys. Chem. Chem. Phys.* **2013**, *15*, 12026.

(32) Harris, R. D.; Bettis Homan, S.; Kodaimati, M.; He, C.; Nepomnyashchii, A. B.; Swenson, N. K.; Lian, S.; Calzada, R.; Weiss, E. A. *Chem. Rev.* **2016**, *116*, 12865.

(33) Chaudhary, Y. S.; Woolerton, T. W.; Allen, C. S.; Warner, J. H.; Pierce, E.; Ragsdale, S. W.; Armstrong, F. A. *Chem. Commun.* **2012**, *48*, 58.

(34) Chai, Z.; Li, Q.; Xu, D. *RSC Adv.* **2014**, *4*, 44991.

(35) Morris-Cohen, A. J.; Frederick, M. T.; Cass, L. C.; Weiss, E. A. *J. Am. Chem. Soc.* **2011**, *133*, 10146.

(36) Manzi, A.; Simon, T.; Sonnleitner, C.; Döblinger, M.; Wyrwich, R.; Stern, O.; Stolarczyk, J. K.; Feldmann, J. *J. Am. Chem. Soc.* **2015**, *137*, 14007.

(37) So, D.; Konstantatos, G. *Chem. Mater.* **2015**, *27*, 8424.

(38) Jin, S.; Tagliazucchi, M.; Son, H.-J.; Harris, R. D.; Aruda, K. O.; Weinberg, D. J.; Nepomnyashchii, A. B.; Farha, O. K.; Hupp, J. T.; Weiss, E. A. *J. Phys. Chem. C* **2015**, *119*, 5195.

(39) Praneeth, V. K. K.; Näther, C.; Peters, G.; Lehnert, N. *Inorg. Chem.* **2006**, *45*, 2795.

(40) Peterson, M. D.; Jensen, S. C.; Weinberg, D. J.; Weiss, E. A. *ACS Nano* **2014**, *8*, 2826.

(41) Bonin, J.; Chaussemier, M.; Robert, M.; Routier, M. *ChemCatChem* **2014**, *6*, 3200.

(42) Chen, L.; Guo, Z.; Wei, X.-G.; Gallenkamp, C.; Bonin, J.; Anxolabéhère-Mallart, E.; Lau, K.-C.; Lau, T.-C.; Robert, M. *J. Am. Chem. Soc.* **2015**, *137*, 10918.

(43) Takeda, H.; Ohashi, K.; Sekine, A.; Ishitani, O. *J. Am. Chem. Soc.* **2016**, *138*, 4354.

(44) Chan, S. L.-F.; Lam, T. L.; Yang, C.; Yan, S.-C.; Cheng, N. M. *Chem. Commun.* **2015**, *51*, 7799.

(45) Rosas-Hernandez, A.; Alsabeh, P. G.; Barsch, E.; Junge, H.; Ludwig, R.; Beller, M. *Chem. Commun.* **2016**, *52*, 8393.

(46) Li, L.; Pandey, A.; Werder, D. J.; Khanal, B. P.; Pietryga, J. M.; Klimov, V. I. *J. Am. Chem. Soc.* **2011**, *133*, 1176.

(47) Lian, S.; Weinberg, D. J.; Harris, R. D.; Kodaimati, M. S.; Weiss, E. A. *ACS Nano* **2016**, *10*, 6372.

(48) Asbury, J. B.; Hao, E.; Wang, Y.; Ghosh, H. N.; Lian, T. *J. Phys. Chem. B* **2001**, *105*, 4545.

(49) Hong, X.; Kim, J.; Shi, S.-F.; Zhang, Y.; Jin, C.; Sun, Y.; Tongay, S.; Wu, J.; Zhang, Y.; Wang, F. *Nat Nano* **2014**, *9*, 682.

(50) Chan, W.-L.; Ligges, M.; Jailaubekov, A.; Kaake, L.; Miaja-Avila, L.; Zhu, X. Y. *Science* **2011**, *334*, 1541.

(51) Knowles, K. E.; Malicki, M.; Weiss, E. A. *J. Am. Chem. Soc.* **2012**, *134*, 12470.

(52) Grodkowski, J.; Behar, D.; Neta, P.; Hambright, P. *J. Phys. Chem. A* **1997**, *101*, 248.

(53) Inoue, H.; Shimada, T.; Kou, Y.; Nabetani, Y.; Masui, D.; Takagi, S.; Tachibana, H. *ChemSusChem* **2011**, *4*, 173.

(54) Chang, X.; Wang, T.; Zhang, P.; Zhang, J.; Li, A.; Gong, J. *J. Am. Chem. Soc.* **2015**, *137*, 8356.

(55) Sun, W.; Qian, C.; He, L.; Ghuman, K. K.; Wong, A. P. Y.; Jia, J.; Jelle, A. A.; O'Brien, P. G.; Reyes, L. M.; Wood, T. E.; Helmy, A. S.; Mims, C. A.; Singh, C. V.; Ozin, G. A. *Nat. Commun.* **2016**, *7*, 12553.

(56) Zhou, R.; Guzman, M. I. *J. Phys. Chem. C* **2014**, *118*, 11649.

(57) Kang, Z.; Tsang, C. H. A.; Wong, N.-B.; Zhang, Z.; Lee, S.-T. *J. Am. Chem. Soc.* **2007**, *129*, 12090.

(58) Sahu, S.; Liu, Y.; Wang, P.; Bunker, C. E.; Fernando, K. A. S.; Lewis, W. K.; Guliants, E. A.; Yang, F.; Wang, J.; Sun, Y.-P. *Langmuir* **2014**, *30*, 8631.

(59) Fujiwara, H.; Hosokawa, H.; Murakoshi, K.; Wada, Y.; Yanagida, S.; Okada, T.; Kobayashi, H. *J. Phys. Chem. B* **1997**, *101*, 8270.

(60) Kauffman, D. R.; Ohodnicki, P. R.; Kail, B. W.; Matranga, C. *J. Phys. Chem. Lett.* **2011**, *2*, 2038.

(61) Manthiram, K.; Beberwyck, B. J.; Alivisatos, A. P. *J. Am. Chem. Soc.* **2014**, *136*, 13319.

(62) Chang, X.; Wang, T.; Gong, J. *Energy Environ. Sci.* **2016**, *9*, 2177.

TOC Figure